A Time Series Generator Modelling Rain Fading

U.-C. Fiebig
Institute of Communications and Navigation, German Aerospace Center (DLR)
P.O. Box 11 16, D-82230 Wessling, Germany
E-mail address: Uwe.Fiebig@dlr.de

1 Abstract

This paper presents a time-series generator for use to model signal attenuation caused be meteorological effects (mainly rain) in satellite-to-Earth or Earth-to-satellite links. The model is based on a mix of a Markov chain like approach and Gaussian random variables. The model can be used in computer simulations and provides a time series whose statistics (distribution of attenuation, distribution of fade durations) are almost identical to those of measured data. The proposed model consists of a generic part and specific parameter sets. These sets depend on the underlying scenario (frequency, climatic zone, elevation of Earth station) and can be changed during the modelling process to consider seasonal and diurnal variations. The paper also shows, how these sets can be created from measured data.

2 Introduction

Numerous statistics on signal attenuation in satellite links due to clouds and precipitation have been published at various conferences like "Ka-Band Utilization Conference", "URSI-F Symposium on Propagation and Remote Sensing", numerous workshops of the Olympus Propagation Experimenters, and within the COST-255 project [1]. These statistics encompass among others the distribution of attenuation, the distribution of fade durations, and the probability of outage [2, 3] and are of great importance to properly design a satellite system, since the fade margin can be determined from these data.

However, fade margin as the only means to compensate for the attenuation due to clouds and precipitation may not be the best way to effectively use the resources. Other fade countermeasures [4] such as adaptive coding and adaptive data rate switching have been proposed [5]. These techniques are referred to as adaptive resource sharing (ARS) because they flexibly allocate resources. ARS considerably outperforms the pure fade margin approach in terms of link availability. The proper design of ARS normally requires computer simulations and computer simulations in turn require a channel model. Such a channel model, however, does not exist so far. This paper closes the gap and proposes a channel model which simulates attenuation due to clouds and precipitation.

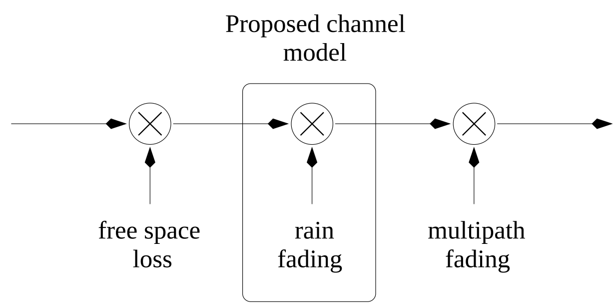

Figure 1: The main sources for attenuation of a signal transmitted from satellite to Earth or vice versa.

The proposed model can be used in addition to those which model fading due to multipath propagation and AWGN. Figure 1 summarizes the main effects causing attenuation on a satellite signal path: Free space loss, rain fading and multipath fading. *Free space loss* defines signal attenuation on a line-of-sight path and depends among others on both carrier frequency and distance between satellite and Earth station [6]. Free space loss may vary in accordance to the orbital position of the satellite. *Rain fading* is understood as signal attenuation due to clouds and precipitation where rain has the greatest significance. Rain fading mainly varies in accordance to the actual rain rate and has a coherence time typically in the order of minutes. *Multipath fading* is caused by interference between two or more versions of the transmitted signal which arrive at the receiver at slightly different times. For satellite transmission multipath fading can be modeled in case of a narrowband scenario as a combination of Rice fading (bad state) and Rayleigh/lognormal fading with shadowing (bad state) [7]. In case of a wideband scenario a tapped delay line model can be used [8]. In contrast to rain fading multipath fading has a substantially smaller coherence time in the order of ms.

When transmitting or receiving with a fixed Earth station multipath fading can often be neglected. However, on a signal path to or from a mobile user both rain fading and multipath fading are present.

3 Measurement Campaign

In most propagation measurement campaigns the received power $r(t)$ of a transmitted beacon or its attenuation $a(t)$ with respect to clear-sky conditions is recorded. We assume that the received signal has not been subjected to multipath fading, which is certainly true as long as the locations of experimental Earth stations are rather exposed.

Recording of the power $r(t)$ of the received signal is carried out in the baseband at a sampling rate $1/T_{rs}$. The samples of $r(t)$ are, thus, obtained every T_{rs} seconds and form the power level time series $r_s(kT_{rs}),\ k = 1, 2, \ldots$, where the unit of $r_s(kT_{rs})$ is decibel (dB). Under clear-sky conditions the received power level r_{cs} is constant (apart from scintillations and AWGN). Both the attenuation $a(t)$ and the attenuation time-series $a_s(kT_{rs}), k = 1, 2, \ldots$ can be written as

$$a(t) = r_{cs} - r(t) , \quad (1)$$

$$a_s(kT_{rs}) = r_{cs} - r_s(kT_{rs}) . \quad (2)$$

We briefly address two well-known statistics which are used in Section 5: (a) The cumulative distribution of attenuation $P_{att}(x)$ which is the probability that – at an arbitrary time instant t_0 – the attenuation due to clouds and precipitation exceeds x dB; (b) the probability $P_{att}(x, \Delta t)$ that – at an arbitrary time instant t_0 – actual attenuation due to clouds and precipitation is part of a fade both lasting longer than Δt and providing always attenuation exceeding x dB. Note that $P_{att}(x, \Delta t)$ is always smaller than $P_{att}(x)$ approaching $P_{att}(x)$ for $\Delta t \to 0$ s. $P_{att}(x)$ and $P_{att}(x, \Delta t)$ are defined as

$$P_{att}(x) = P\{a(t_0) > x\} , \quad (3)$$

$$P_{att}(x, \Delta t) = P\{a(t_0) > x \ \wedge \ t_0 \in [T_a, T_e] \text{ with } (T_e - T_a) \geq \Delta t \ \wedge \ \forall\, t \in [T_a, T_e] : a(t) > x\} . \quad (4)$$

4 Modeling Rain Fading

Basic Requirements

Channel models for mobile radio communications are based on a tapped delay line where the number of delay elements and their corresponding signal attenuation factors can be adjusted to various scenarios (urban, rural, maritime, etc.). Thus, theses models consist of a generic part (the tapped delay line) and specific parameter sets (delay and attenuation factors for each delay line). The specific parameter sets represent the various scenarios.

The channel model for rain fading has been created with the intention to have a similar structure like the above mentioned channel model for mobile radio communications: It consists of a generic part and specific parameter sets. These sets can be adjusted to various conditions such as climatic zone, transmit carrier frequency, elevation angle, season, and time of the day. Another requirement has been that the determination of the specific parameter sets should easily be obtainable from recorded data.

Observations From Recorded Data

An important step towards the proposed channel model was the classification of the recorded data into three types of signal segments, see Figure 2:

- Signal segments of almost constant received power referred to as "C-segments" (C as constant),
- signal segments of more or less monotonously decreasing received power referred to as "D-segments" (D as down), and
- signal segments of more or less monotonously increasing received power referred to as "U-segments" (U as up).

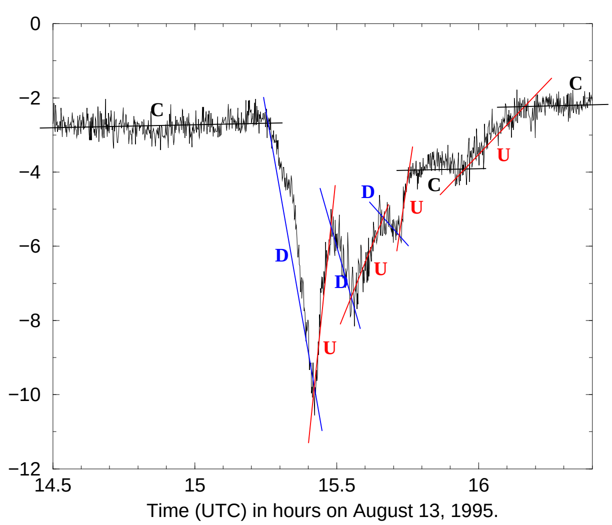

Figure 2: Classification of the received signal $r(t)$ by three types of signal segments: "C", "D", and "U" mean constant, down, and up segment, respectively.

It turned out that the attenuation at a given time instant t_0 strongly depends on the attenuation at "some" time $\Delta\tau$ seconds before and on the actual type of signal segment. Furthermore, it turned out that the measured pdf's of the likelihood $P(y|x)$ have a Gaussian-like shape where $P(y|x)$ is the likelihood that the attenuation is y dB conditioned that it has been x dB $\Delta\tau$ seconds before.

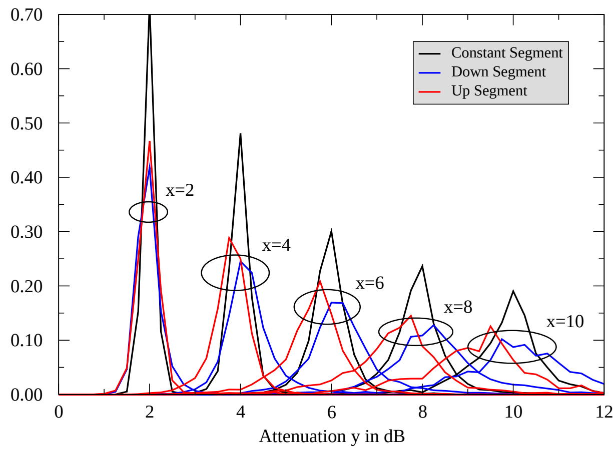

Figure 3: Measured pdf's of $P(y|x)$ for C-, D-, and U-segments and for various values for x.

Figure 3 gives examples of the measured pdf's of $P(y|x)$ for C-, D-, and U-segments, for various values for x and for $\Delta\tau = 64$ s. We see that all pdf's have a quasi-symmetric shape. The pdf's for C-segments provide a maximum at around $y = x$. For D- and U-segments the maxima of the pdf's are located at $y > x$ and $y < x$, respectively. Figure 4 sketches the relation of the pdf of $P(y|x)$ with the type of signal segment exemplarily for a C-segment. We stress that the channel model is based on these pdf's: The time-series generator outputs successive samples where each new sample is a single outcome of a random variable simulating $P(y|x)$.

From Figure 3 we also see that the standard deviations increase with increasing attenuation. This behaviour reflects the dynamics of the channel, which increase with increasing attenuation. We also see that the standard deviations for C-segments are smaller than for D- and U-segments. The reason behind is that C- and D-segments provide inherent dynamics in contrast to C-segments which - by their nature - are segments of more or less constant attenuation.

Channel Model

We introduce the attenuation time-series $y_s(iT_s)$, $i = 1, 2, \ldots$, which represents the output of the channel model. The index i is used instead of k of (2)

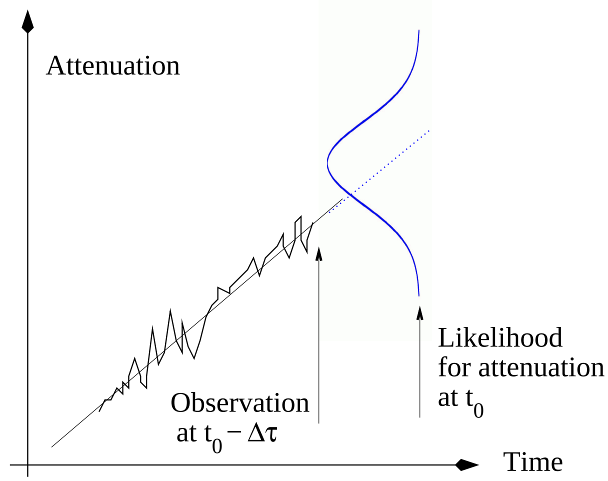

Figure 4: The pdf of $P(y|x)$ for C-segments (increasing attenuation) has a mean value which is larger than the attenuation at $t_0 - \Delta\tau$.

since the sampling rate $1/T_s$ of the channel model may not be identical to the sampling rate $1/T_{rs}$ of the recorded data. Our goal is that $y_s(iT_s)$ and $a_s(kT_{rs})$ provide the same channel statistics defined by (3) and (4).

The generic part of the channel model can be described as follows: It consists of a generator which simulates a Gaussian random variable $\mathbf{z}$ where $\mathbf{z}$ in turn simulates the above introduced pdf's. The outcome of the generator are successive samples forming the time-series $y_s(iT_s)$, $i = 1, 2, \ldots$. Mean value and standard deviation of $\mathbf{z}$ are driven by a previous sample and the actual type of signal segment.

The specific parameter sets of the channel model are

- 3 sets of mean values $\{\mu_j(x)$, $j \in \{C, D, U\}$, $x \in \{1, 2, \ldots\}\}$,
- 3 sets of standard deviations $\sigma_j(x)$, $j \in \{C, D, U\}$, $x \in \{1, 2, \ldots\}\}$,
- T_s, d_1 and d_2.

Above 2 times 3 sets (referred to as family of sets) are obtained from the recorded signal as mean values and standard deviations of the measured pdf's of $P(y|x)$: In accordance with the three types of signal segments we introduce $\mu_C(x)$ and $\sigma_C(x)$ for C-segments, $\mu_D(x)$ and $\sigma_D(x)$ for D-segments, and $\mu_U(x)$ and $\sigma_U(x)$ for U-segments. Note that y_s and x denote attenuation in dB and that all mean values and standard deviations are also measured in dB.

More precisely we can say that $\mu(x)$ and $\sigma(x)$ of $\mathbf{z}$ depend on both the previous sample $x = y_s((i - d_1)T_s)$

and the actual type of signal segment $\Delta(iT_s)$ where $\Delta(iT_s)$ is defined as

$$\Delta(iT_s) = \begin{cases} C \text{ for } |y_s((i-d_1)T_s) - y_s((i-d_2)T_s)| < 1\ dB \\ D \text{ for } y_s((i-d_1)T_s) - y_s((i-d_2)T_s) > 1\ dB \\ U \text{ for } y_s((i-d_1)T_s) - y_s((i-d_2)T_s) < -1\ dB \end{cases} \quad (5)$$

where $d_1 < d_2$. A quantization of y_s in steps of a quarter of a dB seems to be sufficiently accurate. The values for the integers d_1 and d_2 define the time interval which is the basis for the classification of the signal segments. A blockdiagram of the channel model is given in Figure 5.

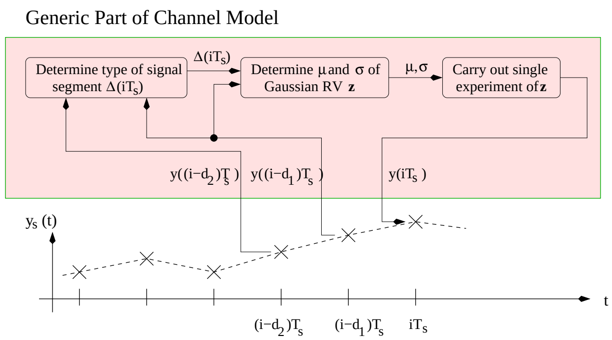

Figure 5: Blockdiagram of the channel model for rain fading for $d_1 = 1$, $d_2 = 2$.

Specific Parameters Sets

The Institute of Communications and Navigation of DLR has carried out a propagation measurement campaign recording the 40 GHz beacon of the Italian satellite ITALSAT with a fixed Earth station. The measurement site is Oberpfaffenhofen, 25 km south-west of Munich. The recorded data is in the form of (2).

For Oberpfaffenhofen (11.3° East, 48.1° North), elevation angle of 34.8°, climatic zone K, carrier frequency 40 GHz, and for an average year we give T_s, d_1, d_2, $\mu_j(x)$, $\sigma_j(x)$, $j \in \{C, D, U\}$. Whereas $\mu_j(x)$ and $\sigma_j(x)$ can be determined directly from the recorded data, the appropriate values for T_s, d_1, d_2 have beed found empirically comparing the statistics on both $P_{att}(x)$ and $P_{att}(x, \Delta t)$ obtained from the channel model to those obtained from recorded data. For the specific channel model we obtained

$$T_s = 64\,s\,, \quad (6)$$

$$d_1 = 1\,, \quad (7)$$

$$d_2 = 2\,. \quad (8)$$

With these specific parameters the channel model produces a time-series where adjacent samples are spaced apart by about 1 minute. The settings of $d_1 = 1$ and $d_2 = 2$ show that the actual type of signal segment depends on two samples which are also separated by about 1 minute. The values of $\mu(x)$ and $\sigma(x)$ are given in Figure 6. It can be seen that $\mu_D(x) > \mu_C(x) > \mu_U(x)$ where the differences increase with increasing x. The mean value $\mu_C(x)$ is close to the function $f(x) = x$ whereas $\mu_U(x) > x$ and $\mu_D(x) < x$. The standard deviations tend to increase with increasing x, cf. Figure 3. This tendency is due to the fact that changes in signal attenuation are the larger the stronger the actual signal attenuation is.

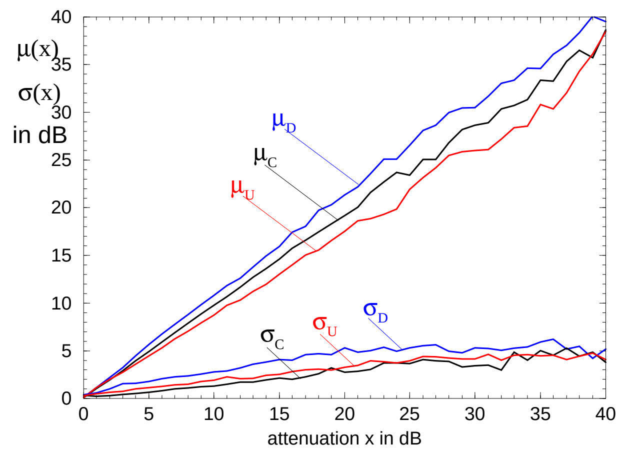

Figure 6: Specific parameter sets from recorded data: $\mu_j(x)$, $\sigma_j(x)$, $j \in \{C, D, U\}$ as a function of x.

It should be mentioned that the channel model inherently provides a transition between the various types of signal segments due to the nature of the Gaussian random variable. Let us assume e.g. that the last samples of the time-series generator form a C-segment at around 1 dB attenuation. From Figure 6 we obtain that for the next experiment $\mu_C(1\,\text{dB}) = 1\,\text{dB}$ and $\sigma_C(1\,\text{dB}) = 0.3\,\text{dB}$. It is not very likely that the outcome is (let us say) 3 dB or more (in terms of attenuation), but if so, the time-series moves over from a C- to a D-segment. The next experiment on **z** will be based on the $\mu_D(3\,\text{dB}) = 3.5\,\text{dB}$ and $\sigma_D(3\,\text{dB}) = 1.5\,\text{dB}$ and so forth.

Finally, we will point out that seasonal and diurnal effects can easily be considered by using different families of sets during the simulation and switching between these families during runtime. E.g. one may work with 4 different families, one family for each season, to consider seasonal variations. Similarly diurnal variations can be considered. We like to point out, that we did not see the need to change T_s, d_1 and d_2 to consider seasonal and diurnal variations

- although the attenuation behaviour is very different [3] - and, thus, expect that other climatic zones or elevation angles may use very similar parameter settings for T_s, d_1 and d_2.

5 Results

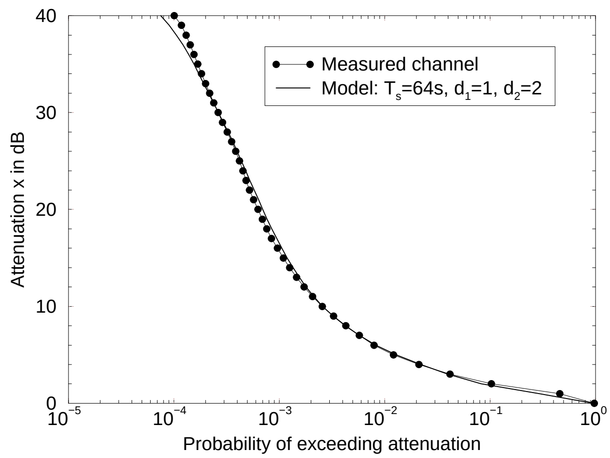

Figure 7: $P_{att}(x)$ as a function of x for the recorded data and for the proposed rain fading channel model.

Figures 7 and 8 reveal that the channel model not only provides the same distribution of attenuation but also the same fade durations. This is an important issue, since fade countermeasures substantially depend on fade durations and not only on the distribution of attenuation. Also other statistics although not shown here such as the probability of outage [2] reveal the suitability of the channel model.

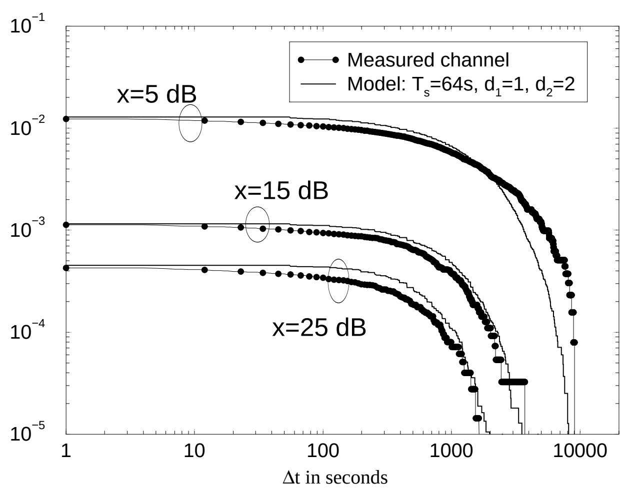

Figure 8: $P_{att}(x, \Delta t)$ as a function of Δt for the recorded data and for the proposed rain fading channel model.

6 Conclusions

A new channel model has been proposed which models signal attenuation due to clouds and precipitation on a satellite-to-Earth or Earth-to-satellite signal path. It has been shown that the channel model is well suited to model rain fading providing an attenuation time-series whose statistics well fit with those of the measured data. We conclude that the channel model is predestinated to test and optimize adaptive fade countermeasures. Specific parameter sets for other scenarios should easily be obtained.

References

[1] http://www.estec.esa.nl/xewww/cost255/

[2] U.-C. Fiebig, M. Schnell: *"40 GHz Measurement Campaign - Evaluation with Respect to System Design and Fade Countermeasures"*, Proc. Fourth European Conference on Satellite Communications (ECSC-4), Rome, Italy, pp. 199-204, November 1997.

[3] U.-C. Fiebig, M. Schnell: *"Impact of Rain Attenuation on Satellite Broadcasting Systems at Ka-band"*, Proc. First International Workshop on Radiowave Propagation Modeling for SatCom Services at Ku-band and above, Noordwijk, The Netherlands, 1998.

[4] L. Castanet, J. Lemorton, M. Bousquet: *"Fade Mitigation Techniques for new Satcom Services at Ku-Band and above: A Review"*, Proc. Fourth Ka Band Utilization Conference, Venice, Italy, pp. 119-127, 2-4 November 1998.

[5] M. Schnell, D. von Hugo: *"Fade Countermeasures and Adaptive Resource Sharing for an Experimental TDMA Satellite Communications System Operating at Ka-Band"*, European Transactions on Telecommunications (ETT), Vol. 9, pp. 561-568, 1998.

[6] G. Maral, M. Bousquet: Satellite Communications Systems. John Wiley & Sons Ltd, UK, 1993.

[7] E. Lutz et al.: *"The land mobile satellite channel recording, statistics and channel model"*, IEEE Trans. on Vehicular Technology VT40, pp. 375-386, 1991.

[8] H. Bischl, A. Jahn, E. Lutz: *"Wideband channel model for UMTS satellite communications - detailed model"*, European Telecommunications Standards Institute, ETSI SMG5 (96), TD 006/96.